Neighboring Pixels Based on a Log-linearized Gaussian Mixture Model for Image Segmentation

Khoa Anh Tran and Gueesang Lee*

Department of Electronics and Computer Science,
Chonnnam National University,
Gwangju, South Korea
anhkhoayy@gmail.com, gslee@chonnam.ac.kr

Abstract. An advanced probabilistic algorithm developed based on log-linearized Gaussian mixture model aims to estimate posteriori probability of neighboring pixel method in image segmentation. We firstly apply the log-linearized Gaussian mixture to develop and determine the mixture and the mixture component of the Gaussian mixture model. Then, the posterior probabilities of each pixel are also identified by using neighboring pixel method. Secondly, employing maximum likelihood technique to simulate the statistic model under our algorithm framework aims to improve accuracy of segmented images and to reduce impacts of noise during image segmentation process. Our research results present good segmentation yields, and the segmented images are more accuracy comparing to the segmented images which obtained by other segmentation methods.

Keywords: Neighboring pixels, Log-linearized, Gaussian Mixture Model (GMM), Image Segmentation, Maximum Likelihood.

1 Introduction

Today, color image segmentation is useful in many applications in image processing and image recognition systems. The good segmentation results would help to identify regions of interest and objects in the scenes that is very beneficial to the subsequent image analysis or annotation. For example, many communication tasks require high compression ratio to save network resource. One possible way to realize the higher compression ratio is to discriminate objects in an image and compress only the targeted objects toward user's concerns. This makes image segmentation extremely important role in providing the necessary information. Several previous works have been carrying out for image segmentation by using threshold method [1]. However, it is not easy to determine and identify a proper threshold value. This is also the large disadvantage to threshold method, and in some cases a bad choice of a certain thresholds could alternate the quality of the segmentation and probably leads to a worse interpretation. An artificial neutral network is an approach applied in image

* Corresponding author.

I. Zelinka et al. (eds.), *AETA 2013: Recent Advances in Electrical Engineering and Related Sciences*, Lecture Notes in Electrical Engineering 282,
DOI: 10.1007/978-3-642-41968-3_32,

segmentation in order to avoid this disadvantage. In the paper [2], the authors applied a feature vectors that are extracted from an image using a neural network. This method and model simulation do not place out spatial information, the spatial attributes of pixels are maximally used in this method. This method would help to minimize the distance between the feature vectors. The experiment results indicate that this method work well and lead to sub-optimal image segmentation.

Recently, with the expansion application of Gaussian mixture model (GMM), image segmentation based on GMM has become popular [3].In this approach a mixture of multi-variant densities and the mixture parameters are estimated by using EM algorithm. However, a main drawback of this method is that the number of Gaussian mixture components is assumed known as prior, resulting not sensitive to noise of segmentation. The spatially variant finite model was proposed in [4]. In this model a maximum-a-posteriori (MAP) estimation is determined by using Markov random fields (MRF). The main advantage of MRF models is that prior information of the pixel labels can be imposed locally through clique potentials. Importantly, segmentation accuracy is quite sensitive to the initialization of segmentation algorithm, because of using the local optimization parameter estimation algorithms such as EM. Therefore, the initializations for these local algorithms have to be well selected and determined. This approach works well in minimizing the impacts of noise though the image segmentation process.

An advanced algorithm based on the GMM and the log-linear model is necessarily to be developed to improve image segmentation. Therefore our study objectives aim: 1) applying the log-linear model to a product of the mixture coefficient and the mixture component of the GMM. 2) using the local spatial interactions between neighboring pixels to reduce impacts of noise in image segmentation. The proposed method will be applied for segmenting synthetic and real world grayscale images. The robustness, accuracy and effectiveness of proposed model and other methods such as standard GMM, and K-means, and Mean-shift are compared to evaluate the advantages of the proposed method.

This paper is organized as follows. In section 2, the segmentation algorithm for image is presented. In section 3, the experimental results are presented and discussed. Finally, the conclusions are given in section 4.

2 Proposed Approach

2.1 Neighboring Pixels

In this paper, we use the local spatial interaction between neighboring pixels in a 3×3 window. For each of the ith window, neighboring pixels are denoted by

$$X = (x_1x_1, x_1x_2, \ldots, x_1x_d, x_2x_2, x_2x_3, \ldots, x_2x_d, \ldots, x_dx_d) \tag{1}$$

where x_2x_2 is the central pixel of *k*-th window and $x_1x_1, x_1x_2, x_1x_3, x_2x_1, x_2x_3, x_3x_1, x_3x_2, x_3x_3$ are called the neighboring pixels of the x_2x_2.

For each window, the posterior probability $P(k \mid x)$ for all classes. with the central pixel x_2x_2 will belong to an certain class that has the largest posterior probability.

2.2 Log-linearized Gaussian Mixture Model

Here, a PDF $f(x)$ of a feature vector $x \in \Re^d$ is represented by a GMM with K classes:

$$f(x) = \sum_{k=1}^{K} \sum_{m=1}^{M_k} \alpha_{k,m} g(x; \mu^{(k,m)}, \Sigma^{(k,m)}) \tag{2}$$

$$\sum_{k=1}^{K} \sum_{m=1}^{M_k} \alpha_{k,m} = 1 \tag{3}$$

$$\begin{aligned} g(x; \mu^{(k,m)}, \Sigma^{(k,m)}) &= (2\pi)^{-\frac{d}{2}\left|\Sigma^{(k,m)}\right|^{-\frac{1}{2}}} \\ &\times \exp\left[-\frac{1}{2}(x_2x_2 - \mu^{(k,m)})^T (\Sigma^{(k,m)})^{-1} (x_2x_2 - \mu^{(k,m)})\right] \end{aligned} \tag{4}$$

where $M_k (k = 1,...K)$ denotes the number of components of the class $k; \alpha_{k,m}$ denotes a mixture coefficient or a mixing proportion of each component $\{k, m\}$ and $\mu^{(k,m)} \in \Re^d$ and $\Sigma^{(k,m)} \in \Re^{d \times d}$ d represent the mean vector and the covariance matrix of each component $\{k, m\}$. Note that $|.|$ represents the determinant.

Let us consider a problem to classify an observed vector x into one of K classes. The Bayes decision theory determines a specific class if a posteriori probability of the vector belonging to the class is larger than the ones to any other classes. Using the GMM of the PDF of x, the posteriori probability $P(k \mid x)(k = 1,...K)$ is given as

$$P(k \mid x) = \sum_{k=1}^{K} P(k, m \mid x) = \sum_{m=1}^{M_k} \frac{P(k,m)P(x, x \mid k, m)}{P(x)} \tag{5}$$

where P(k, m) is the a priori probability of the class k and the component m, which corresponds to the mixing coefficient $\alpha_{k,m}$; and $P(x \mid k, m)$ is the PDF of x conditioned by the class k and the component m. Then, using Eq. (l), the posteriori probability $P(x \mid k, m)$ can be expressed as

$$P(k,m\mid x)=\frac{P(k,m)P(x\mid k,m)}{\sum_{k'=1}^{K}\sum_{m'=1}^{M_{k'}}P(k'\mid m')P(x\mid k',m')}$$

$$=\frac{\alpha_{k,m}g(x;\mu^{(k,m)},\Sigma^{(k,m)})}{\sum_{k'=1}^{K}\sum_{m'=1}^{M_{k'}}\alpha_{k',m'}g(x;\mu^{(k',m')},\Sigma^{(k',m')})} \tag{6}$$

Since $g(x;\mu^{(k,m)},\Sigma^{(k,m)})$ is the d-dimensional Gaussian distribution given as Eq. (3), using the mean vector $\mu^{(k,m)}=(\mu_1^{(k,m)},\ldots\},\mu_d^{(k,m)})^T$ and the inverse of the covariance matrix $\Sigma^{(k,m)-1}=[s_{ij}^{(k,m)}]$, the numerator of the right side of Eq. (5) can be represented as $\alpha_{k,m}g(x;\mu^{(k,m)},\Sigma^{(k,m)})$

$$\begin{aligned}&g(x;\mu^{(k,m)},\Sigma^{(k,m)})\\&=\exp[-\frac{1}{2}\sum_{j=1}^{d}\sum_{l=1}^{j}(2-\delta_{jl})s_{jl}^{(k,m)}x_jx_l+\sum_{j=1}^{d}\sum_{l=1}^{d}s_{jl}^{(k,m)}\mu_j^{(k,m)}x_l\\&-\frac{1}{2}\sum_{j=1}^{d}\sum_{l=1}^{j}\delta_{jl}s_{jl}^{(k,m)}\mu_j^{(k,m)}\mu_l^{(k,m)}-\frac{1}{2}\log|\Sigma^{(k,m)}|+\log\alpha_{(k,m)}]\end{aligned} \tag{7}$$

where δ_{jl} is the Kronecker delta: $\delta_{ij}=1$ when $i=j$ and $\delta_{ij}=0$ when $i\neq j$. Let us consider to linearize the right side of Eq. (6). Taking a logarithm of Eq. (6), we can get

$$\zeta_{k,m}\triangleq\log\alpha_{(k,m)}g(x;\mu^{(k,m)},\Sigma^{(k,m)})=\beta^{(k,m)^T}X\ \ldots\ldots \tag{8}$$

Where $X\in\Re^H$ and $\beta^{(k,m)}\in\Re^H$ are defined as from Eq. (1)

$$\begin{aligned}&X=(x_1x_1,x_1x_2,\ldots,x_1x_d,x_2x_2,x_2x_3,\ldots,x_2x_d,\ldots,x_dx_d)\\&\beta^{(k,m)}=(\beta_0^{(k,m)},\sum_{j=1}^{d}s_{jl}^{(k,m)}\mu_j^{(k,m)},\ldots,\sum_{j=1}^{d}s_{jd}^{(k,m)}\mu_j^{(k,m)}\\&-\frac{1}{2}s_{l1}^{(k,m)},-s_{l2}^{(k,m)},-s_{ld}^{(k,m)},\ldots,-\frac{1}{2}s_{dd}^{(k,m)})^T\end{aligned} \tag{9}$$

$$\beta_0^{(k,m)} = -\frac{1}{2}\sum_{j=1}^{d}\sum_{l=1}^{j}\delta_{jl}s_{jl}^{(k,m)}\mu_j^{(k,m)}\mu_l^{(k,m)} - \frac{d}{2}\log 2\pi - \frac{1}{2}\log|\Sigma^{(k,m)}| + \log\alpha_{(k,m)} \tag{10}$$

And the dimensionally is H defined as $H = 1 + d(d+3)/2$. We can see that $\zeta_{k,m}$ can be expressed as a product of the coefficient vector $\beta^{(k,m)}$ and the modified input vector $X \in \Re^H$.

However, since $\sum_{k=1}^{K}\sum_{m=1}^{M_k} P(k,m \mid x) = 1$, the variable is $\zeta_{k,m}$ redundant. Then, a new variable $Y_{k,m}$ and a new coefficient vector $w^{(k,m)} \in \Re^H$ are introduced:

$$Y_{k,m} \triangleq \zeta_{k,m} - \zeta_{M,M_k} = (\beta^{(k,m)} - \beta^{(K,M_k)^T})X = w^{(k,m)}X \tag{11}$$

where $w^{(K,M_k)} = 0$. It should be noted that $w^{(k,m)}$ becomes a weight coefficient with no constraints. Then the posterior probability

$$P(k,m \mid x) = \frac{\exp[Y_{k,m}]}{\sum_{k'=1}^{K}\sum_{m'=1}^{M_k}\exp[Y_{k',m'}]} \tag{12}$$

As mentioned above, by taking a logarithm of the PDF of each component, the posterior probability can be expressed using the variable $Y_{k,m}$ that is a linear sum of the modified input vector X and the coefficient vector $w^{(k,m)}$: that is, the GMM is log-linearized.

Using the data image, a log-likelihood function L can be derived as

$$E = -\ln L - \sum_{k=1}^{K}\ln\left\{\sum_{m=1}^{M_k} g(x;\mu^{(k,m)},\Sigma^{(k,m)})P(k,m \mid x)\right\} \tag{13}$$

3 Experimental Results

In this section, we evaluate the segmentation performance of the proposed algorithm by using a subset of the Berkeley image segmentation dataset and benchmark [8] (Fig. 1). This benchmark dataset consists of a set of natural images along with their ground truth segmentation maps which were provided by different individuals. In this experiment, we employ the probabilistic rand (PR) index [9] to quantitatively evaluate the performance of the proposed algorithm. Let $GT = \{GT_1, GT_2, ..., GT_k\}$ denote a set of ground truth images and G the segmentation result to be evaluated the PR index is given by

$$PR(G_s, GT) = \frac{2}{M(M-1)} \sum_{\substack{i,j \\ i<j}} [c_{ij} p_{ij} + (1 - c_{ij})(1 - p_{ij})] \tag{14}$$

where c_{ij}=1 if pixels i and j belong to the same class in Gs, otherwise. M is the number of image pixels, and is the ground truth probability of pixels i and j belong to the same class. The PR index takes values between 0 and 1 with the values close to 1 means a good segmentation result, and close to 0 means a bad result. Unnikrishnan and Hebert in [10] have proved that the PR index is robust to segmentation maps resulting from ground truth segment splitting or merging.

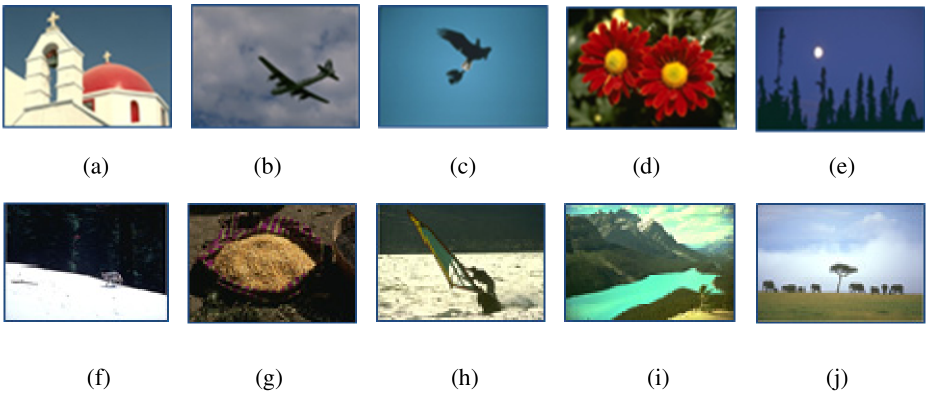

Fig. 1. Images from the Berkeley's image segmentation dataset. (a) 118035, (b) 2096, (c) 135069, (d) 124084, (e) 238011, (f) 167062, (g) 58060, (h) 62096, (i) 176035, (j) 253036.

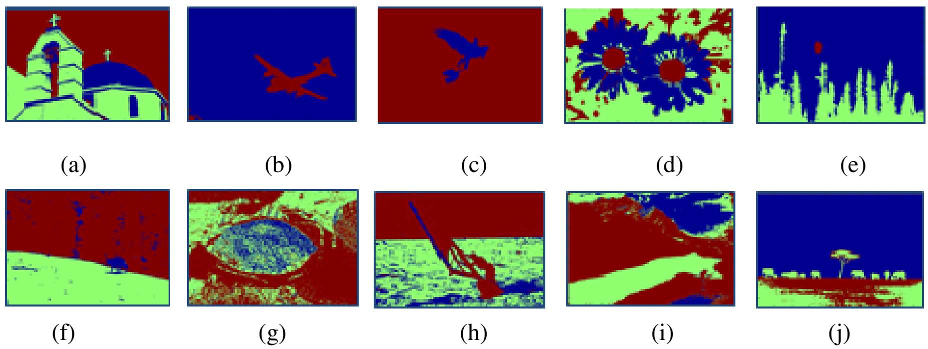

Fig. 2. Image segmentation results obtained by employing the proposed method. (a) 118035, (b) 2096, (c) 135069, (d) 124084, (e) 238011, (f) 167062, (g) 58060, (h) 62096, (i) 176035, (j) 253036.

Figure 3 presents the segmentation results obtained from our proposed method and 4 other methods by using the real world image as the input.

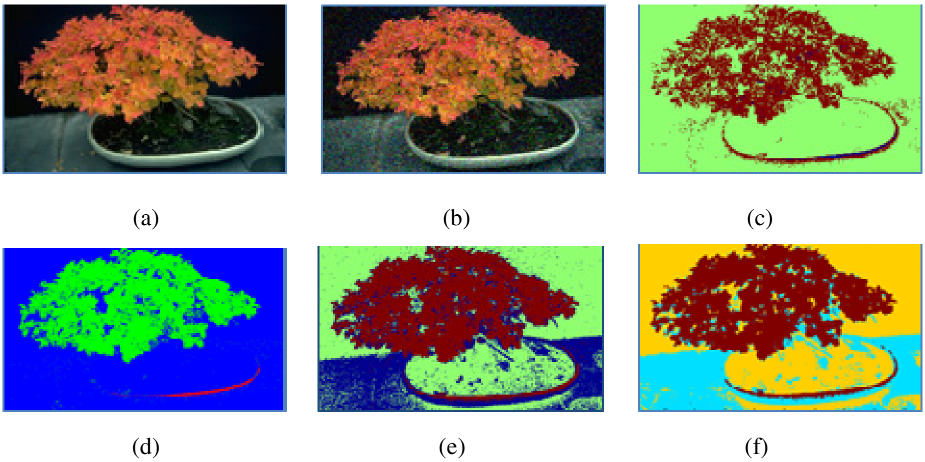

Fig. 3. 481x321 color testing data, (a) Original image, (b) Standard deviation of Gaussian noise (0 mean, 0.001 variance), (c) K-means (PR=0.670), (d) Mean shift (PR=0.691), (e) Standard GMM (PR=0.723), (f) Our method (PR=0.8184).

Table 1. The PR indexes of segmentation applying our proposed method and other 4 methods on Berkeley images

PR indexes					
Image	k	K-means	Mean-shift	Standard GMM	The proposed algorithm
118035	3	0.624	0.688	0.706	0.784
2096	2	0.980	0.980	0.982	0.984
135069	2	0.983	0.983	0.983	0.985
124084	3	0.520	0.624	0.663	0.730
238011	3	0.714	0.769	0.800	0.815
167062	3	0.630	0.635	0.720	0.786
58060	3	0.552	0.588	0.596	0.605
62096	3	0.601	0.615	0.628	0.642
176035	3	0.754	0.760	0.769	0.771
253036	3	0.630	0.635	0.635	0.660
Mean	-	0.688	0.727	0.748	0.762

Table 1 presents the PR values indicating the efficiencies of image segmentation obtained from our proposed algorithm and from other algorithms, namely K-means, Mean-shift and Standard GMM. These show that using the same number of segmentation, presented in Eq. 8, the PR values obtained from our method is slightly higher than the PR values obtained from other methods for the same tested images. Importantly, by comparing the images in Figure 1 and 2, our method results in Figure 2 show that the developed algorithm is efficiently applied for image segmentation at different class regions results, as well as can preserve well boundary information for all cases.

In another experiment, our method is tested robustness and efficacy with 10 iterations though the segmentation process, and the testing process is implemented by adding noise into the original images. Figure 3 presents the image segmentation results of our research method and other methods for the same one image extracted from the Berkeley Segmentation Dataset. Figure 3a shows the original image with 3 classes. Figure 3b is the result that obtained by using Gaussian noise (0 mean, 0.001 variance). Figure (3c-3e) present results obtained from 3 methods (with 15 iterations for each method). Figure 3f presents our study result. Although the tested images during our experiment process are somehow degraded by adding high levels of noise, the results show that our method provides better images than other methods. Moreover, our proposed method demonstrates robustness with respect to noise yielding a better segmentation result.

4 Conclusions

In this paper, we proposed a new mixture model based on the log-linerarized Gaussian mixture model, which can estimate the posterior probability for image segmentation. Here we have presented experimental results of the proposed model and also presented a comparison of image segmentation results between our method and three other algorithms to validate our research method. Experimental results show that the proposed algorithm has generally satisfying properties for image segmentation, and it outperforms the competing algorithms in terms of robustness to efficiency and preservation of target boundary information. Finally, in this paper, the number of classes (K) is manually selected. In the future, we would like to further our study on how to automatically optimize this parameter.

Acknowledgments. This work was supported by the National Research Foundation of Korea (NRF) grant funded by the Korea government (MEST)(2013-006535). Also this research was supported by the MSIP (Ministry of Science, ICT&Future Planning), Korea, under the ITRC (Information Technology Research Center) support program (NIPA-2013-H0301-13-3005) supervised by the NIPA (National IT Industry Promotion Agency).

References

[1] Glasbey, C.A.: An Analysis of Histogram-based Thresholding Algorithm. CVGIP: Graphical Model and Image Processing 55, 532–537 (1993)

[2] Amartur, S.C., Piraino, D., Takefuji, Y.: Optimization neural networks for the segmentation of magnetic resonance images. IEEE Transaction on Medical Imaging 11, 215–220 (1992)

[3] MacLanchlan, G., Peel, D.: Finite Mixture Models. John Wiley and Sons, New York (1997)
[4] Sanjay-Gopal, S., Hebert, T.: Bayseian pixel classification using spatially variant finite mixtures and the generalized EM algorithm. IEEE Trans. Image Process. 7(7), 1–14 (1998)
[5] Gonzalez, R., Woods, R.E.: Digital Image Processing, 3rd edn. Pearson (2010)
[6] Tosuji, T., Ichinobe, H., Fukuda, O., Kaneko, M.: A Maximum Likelihood Neural Network Based on a Log-linearized Gaussian Mixture Model. In: Proc. IEEE Conf. Neural Network, vol. 3, pp. 1293–1298 (1995)
[7] Bishop, C.M.: Pattern Regconition and Machine Learning, pp. 240–242. Springer (2006)
[8] Martin, D., Fowlkes, C., Tal, D., Malik, J.: A database of human segmented natural images and its application to evaluating segmentation algorithms and measuring ecological statistics. In: Proc. Int. Conf. Comp Vision, Canada, pp. 416–423 (July 2001)
[9] Unnikrishnan, R., Pantofaru, C., Hebert, M.: A measure for objective evaluation of image segmentation algorithms. In: Proc. IEEE Conf. Comp. Vis. Pattern Recog., vol. 3, pp. 34–41 (June 2005)
[10] Unnikrishnan, R., Hebert, M.: Measures of similarity. In: Proc. IEEE Workshop Comput. Vis. Appl., pp. 394–400 (January 2005)